

# A Performance Consideration of $C^1$ -Continuous Thin Beam Element

Yong-woo Kim\* and Oak-key Min\*\*

(Received December 2, 1992)

The performance of  $C^1$ -continuous thin beam element is considered by using the error-moment equations derived from the energy functional. The analysis shows explicitly that the rigid body motions of a thin beam can be described correctly; and that the Barlow's optimal stress points are re-interpreted as the optimal points in the limit sense, that is, true bending moment points and true shear force points converge to their optimal points respectively as the number of elements increases, on which examples are illustrated.

**Key Words:** Error-Moment Equations, Optimal Point, True Bending Moment Points, True Shear Force Point, True Resultant Forces' Points

## 1. Introduction

During the last two decades, some theoretical methods have been proposed to estimate the error of the solutions of displacement-based finite element method which employs polynomial functions for representation of displaced shapes. Moan(1973) has shown that the finite element approximation of principal derivatives in the energy functional is of least squares type and that the approximation of derivatives takes place almost independently with each element. He utilized the nature of the least squares approximation to predict points within an element where the error in principal derivatives of the energy functional is minimal. Hinton and Campbell(1974) have suggested reduced integration technique by considering the problem of smoothing the numerically discontinuous model of a physically continuous system. Barlow(1976) attempted to rationalize the reasons for the presence of optimal stress points at which the stresses have the same degree of accuracy as the nodal displacements. He also

outlined a process by which the location of such points may be determined. All the above theoretical arguments are based on the fact that the FE procedure provides a weighted least-squares fit. Min and Kim(1991) have suggested 'reduced minimization theory' for establishing the unified viewpoint on spurious constraints and spurious zero energy modes of  $C^0$ -continuous elements. By using the theory, they obtained the optimal stress points for each strain component of displacement-coupled problems and rationalized the selective reduced integration techniques. And they explained the relationship between spurious constraints and spurious zero energy modes by using the theory, which is based on the concept of field-consistency.

In this paper, by applying the reduced minimization theory to  $C^1$ -continuous beam element, the validity of their theory in  $C^1$ -continuous elements as well as  $C^0$ -continuous elements will be shown-specifically speaking, the descriptive capability for rigid body motions of beam and the descriptive capability for deformations (deflection and slope) and resultant forces (bending moment and shear force) are examined by using the theory. In addition to it, we will re-interpret the optimal stress points of  $C^1$ -continuous beam element. To do these, we will illustrate various applications of the error-moment equations to

\* Department of Mechanical Engineering, College of Engineering, Sunchon National University

\*\* Department of Mechanical Design and Production Engineering, College of Engineering, Yonsei University

thin beam element.

## 2. Error-Moment Equation

### 2.1 Euler-Bernoulli beam theory

If the transverse deflection of a thin beam as shown in Fig. 1 is denoted by  $w$ , the slope( $\theta$ ) and the curvature( $\chi$ ) of the beam are expressed respectively by

$$\theta = dw/dx, \tag{1}$$

$$\chi = d\theta/dx, \tag{2}$$

where the  $x$  is the coordinate along the neutral axis of the beam.

The bending moment( $M$ ) and shear force( $V$ ) at any section are given by

$$M = EI\chi, \tag{3}$$

$$V = dM/dx, \tag{4}$$

respectively, where  $E$  is Young's modulus and  $I$  is the 2nd moment of the cross-section.

The total potential energy of the beam is given by

$$I = \frac{EI}{2} \int_L (\chi)^2 dx + W_p, \tag{5}$$

where  $W_p$  is the potential of externally applied loads.

### 2.2 Error-moment equation

According to Zienkiewicz, the minimization of the functional given by Eq. (5) is equivalent to the minimization of  $I^*$  such as

$$I^* = \frac{EI}{2} \int_L (\chi - \chi_{\text{exact}})^2 dx, \tag{6}$$

in which  $\chi_{\text{exact}}$  is the exact curvature.

If we approximate the deflection( $w$ ) and the slope( $\theta$ ) by the Hermite polynomials of degree  $M = n + r - 1$ , [i. e., we shall approximate the deflection by a polynomial of degree  $n + r - 1$  passing through  $w(x_j)$ ,  $j=1, 2, \dots, n$  and having

derivatives  $w'(x_j) = \theta(x_j)$ ,  $j=1, 2, \dots, r$ ] then the approximate displacement is expressed as

$$w(x) = \sum_{j=1}^n h_j(x)w(x_j) + \sum_{j=1}^r \bar{h}_j(x)\theta(x_j), \tag{7}$$

where  $h_j(x)$  and  $\bar{h}_j(x)$  are the Hermite polynomials of degree  $M = n + r - 1$ . So the approximate deflection has to be a polynomial of degree  $M$  and it may be expressed as follows.

$$w(x) = \sum_{i=0}^M a_i x^i, \tag{8}$$

$$= a_0 + a_1 x + a_2 x^2 + a_3 x^3 + \dots + a_M x^M,$$

where  $a_i$  ( $i=0, 1, \dots, M$ ) are the generalized coordinates of deflection. Therefore, the approximate slope and the approximate curvature are expressed as

$$\theta(x) = L_1 w(x) \text{ (where } L_1 = d[\cdot]/dx), \tag{9}$$

$$= a_1 + 2a_2 x + 3a_3 x^2 + \dots + Ma_M x^{M-1},$$

and

$$\chi(x) = L_2 w(x) \text{ (where } L_2 = d^2[\cdot]/dx^2), \tag{10}$$

$$= 2a_2 + 6a_3 x + 12a_4 x^2 + \dots + (M)(M-1)a_M x^{M-2},$$

respectively.

By substituting the approximate curvature into the functional  $I^*$  in Eq. (6), the functional  $I^*$  may be expressed as

$$I^*(a_0, a_1, a_2, a_3, \dots, a_M) = \int_L \left( L_2 \sum_{i=0}^M a_i x^i - \chi_{\text{exact}} \right)^2 dx. \tag{11}$$

For the functional  $I^*$  to be minimum,  $\delta I^* = 0$  should be satisfied This minimization is performed equivalently by

$$\frac{\partial I^*}{\partial a_k} = 0, \quad k=0, 1, 2, \dots, M, \tag{12}$$

which produces

$$\int_L (x - \chi_{\text{exact}}) L_2 x^k dx = 0, \quad k=0, 1, \dots, M. \tag{13}$$

The Eq. (13) is called error-moment equations since Eq. (13) requires that the moment of  $(x - \chi_{\text{exact}})$ , from 0-th one up to  $L_2 x^M$ -th one, be zero. Min and Kim(1991) have shown that the error-moment equations give a set of constraints imposed on a single unconstrained element.

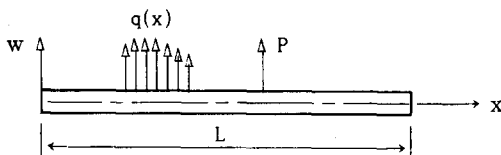


Fig. 1 Euler-Bernoulli beam

### 3. Application of Error-Moment Equation

The error-moment equation is effective to analyze the characteristics or performance of an element. In this section, we will apply the error-moment equation to a single unconstrained  $C^1$ -continuous Euler-Bernoulli beam element which employs the Hermite polynomials of degree three in order to examine its descriptive capability of rigid body motion, deformation, bending moment, and shear force.

The deflection interpolated by using the first-order Hermite polynomials is

$$w(x) = a_0 + a_1x + a_2x^2 + a_3x^3, \quad (14)$$

and the corresponding approximate slope and curvature are given as

$$\theta(x) = a_1 + 2a_2x + 3a_3x^2, \quad (15)$$

$$\chi(x) = 2a_2 + 6a_3x, \quad (16)$$

respectively.

The error-moment equations for a single element shown in Fig. 2 are written as

$$\int_{-0.5L}^{+0.5L} (\chi - \chi_{\text{exact}}) dx = 0, \quad (17)$$

and

$$\int_{-0.5L}^{+0.5L} (\chi - \chi_{\text{exact}}) x dx = 0. \quad (18)$$

First, consider the descriptive capability for rigid body motions. To do this, suppose that the external loads are zero so that  $\chi_{\text{exact}} = 0$ . Then the error-moment equations in Eqs. (17) and (18) yield two constraints such as

$$a_2 = 0 \text{ and } a_3 = 0. \quad (19)$$

By substituting Eq. (19) into Eqs. (14, 15, 16), the quantities are expressed as follows.

$$w(x) = a_0 + a_1x, \quad (20)$$

$$\theta(x) = a_1, \quad (21)$$

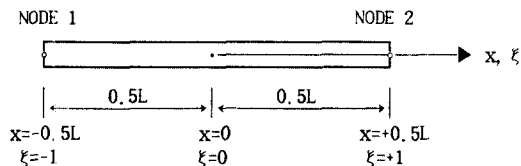


Fig. 2 A single beam element

$$\chi(x) = 0. \quad (22)$$

The Eqs. (20, 21, 22) describe the deformation state of the element under zero-loading. Exactly speaking, Eqs. (20, 21, 22) describe the two rigid body modes of the single unconstrained beam element; one is the transverse translation, and the other is the rotation in the plane of paper in Fig. 2. These rigid body motions coincide with those of the beam theory, so there does not exist spurious rigid body motions.

Now, consider the deformation of the single element shown in Fig. 2 when the beam is subject to constant, linear, quadratic, cubic, or quartic curvature field.

(1) When the curvature is constant, i. e.,  $\chi_{\text{exact}} = b_0 = (\text{const.})$ ;

The error of approximate curvature is

$$\begin{aligned} \chi - \chi_{\text{exact}} &= (2a_2 - b_0) + 6a_3x, \\ &= A_0 + A_1x. \end{aligned} \quad (23)$$

The error-moment equations in Eqs. (17) and (18) yield the constraints such as

$$A_0 = 0 \text{ and } A_1 = 0.$$

Thus

$$M - M_{\text{exact}} = EI(\chi - \chi_{\text{exact}}) = 0, \quad (24)$$

$$V - V_{\text{exact}} = d(M - M_{\text{exact}})/dx = 0, \quad (25)$$

which means that the approximate resultant forces are identical with the exact ones at all points within the element. Therefore, the approximate deformation fields may be exact.

(2) When the curvature is linear, i. e.,  $\chi_{\text{exact}} = b_0 + b_1x$ ;

The error of approximate curvature is

$$\begin{aligned} \chi - \chi_{\text{exact}} &= (2a_2 - b_0) + (6a_3 - b_1)x, \\ &= A_0 + A_1x, \end{aligned} \quad (26)$$

and from the error-moment equations in Eqs. (17) and (18), we obtain the constraints

$$A_0 = 0 \text{ and } A_1 = 0.$$

Therefore

$$M - M_{\text{exact}} = EI(\chi - \chi_{\text{exact}}) = 0, \quad (27)$$

$$V - V_{\text{exact}} = d(M - M_{\text{exact}})/dx = 0, \quad (28)$$

which means that all the approximate quantities are identical with exact ones like the beam with constant curvature field.

(3) When the curvature is quadratic, i.e.,  $\chi_{\text{exact}} = b_0 + b_1x + b_2x^2$ ;

The error of approximate curvature is

$$\begin{aligned} \chi - \chi_{\text{exact}} &= (2a_2 - b_0) + (6a_3 - b_1)x + (-b_2)x^2, \\ &= A_0 + A_1x + A_2x^2. \end{aligned} \quad (29)$$

Thus, the error-moment equations yield the constraints such as

$$A_0 = -(A_2/3)(L/2)^2 \text{ and } A_1 = 0.$$

Therefore

$$\begin{aligned} M - M_{\text{exact}} &= EI(\chi - \chi_{\text{exact}}), \\ &= A_2EI\{x^2 - (1/3)(L/2)^2\}, \quad (30) \\ V - V_{\text{exact}} &= d(M - M_{\text{exact}})/dx, \\ &= 2A_2EIx, \quad (31) \end{aligned}$$

which imply that the approximate bending moment coincides with the exact one only at the points of  $x = \pm(1/3)^{0.5}(L/2)$  and that the approximate shear force is exact only at the origin  $x = 0$ . Note that the points of  $x = \pm(1/3)^{0.5}(L/2)$  are identical with Gauss points and that they are located symmetrically with respect to the origin.

(4) When the curvature is cubic, i.e.,  $\chi_{\text{exact}} = b_0 + b_1x + b_2x^2 + b_3x^3$ ;

The error of approximate curvature is

$$\begin{aligned} \chi - \chi_{\text{exact}} &= (2a_2 - b_0) + (6a_3 - b_1)x \\ &\quad + (-b_2)x^2 + (-b_3)x^3, \\ &= A_0 + A_1x + A_2x^2 + A_3x^3, \end{aligned} \quad (32)$$

and the error-moment equations yield the constraints such as

$$\begin{aligned} A_0 &= -(A_2/3)(L/2)^2 \text{ and} \\ A_1 &= -(3A_3/5)(L/2)^2. \end{aligned}$$

Therefore

$$\begin{aligned} \chi - \chi_{\text{exact}} &= A_2\{x^2 - (1/3)(L/2)^2\} \\ &\quad + A_3x\{x^2 - (3/5)(L/2)^2\}, \quad (33) \\ M - M_{\text{exact}} &= EI[A_2\{x^2 - (1/3)(L/2)^2\} \\ &\quad + A_3x\{x^2 - (3/5)(L/2)^2\}], \quad (34) \\ V - V_{\text{exact}} &= EI[2A_2x + A_3x\{3x^2 - (3/5) \\ &\quad (L/2)^2\}], \quad (35) \end{aligned}$$

from which we see that  $(M - M_{\text{exact}}) = 0$  may not have certain symmetrical roots with respect to the origin, where approximate bending moments are identical with exact ones, as long as  $A_3$  in Eq. (34) is not zero. Also, we see that  $x = 0$  will never be a root of  $(V - V_{\text{exact}}) = 0$  as long as  $A_3$  is not

zero.

(5) When the curvature is quartic, i.e.,  $\chi_{\text{exact}} = b_0 + b_1x + b_2x^2 + b_3x^3 + b_4x^4$ ;

The error of approximate curvature is

$$\begin{aligned} \chi - \chi_{\text{exact}} &= (2a_2 - b_0) + (6a_3 - b_1)x + (-b_2)x^2 \\ &\quad + (-b_3)x^3 + (-b_4)x^4, \\ &= A_0 + A_1x + A_2x^2 + A_3x^3 + A_4x^4. \end{aligned} \quad (36)$$

So, the error-moment equations yield constraints such as

$$\begin{aligned} A_0 &= -(A_2/3)(L/2)^2 - (A_4/5)(L/2)^4 \text{ and} \\ A_1 &= -(3A_3/5)(L/2)^2. \end{aligned}$$

Thus

$$\begin{aligned} \chi - \chi_{\text{exact}} &= A_2\{x^2 - (1/3)(L/2)^2\} \\ &\quad + A_3x\{x^2 - (3/5)(L/2)^2\} \\ &\quad + A_4\{x^4 - (1/5)(L/2)^4\}, \end{aligned} \quad (37)$$

$$\begin{aligned} M - M_{\text{exact}} &= EI[A_2\{x^2 - (1/3)(L/2)^2\} \\ &\quad + A_3x\{x^2 - (3/5)(L/2)^2\} \\ &\quad + A_4\{x^4 - (1/5)(L/2)^4\}], \end{aligned} \quad (38)$$

$$\begin{aligned} V - V_{\text{exact}} &= EI[2A_2x + A_3\{3x^2 - (3/5)(L/2)^2\} \\ &\quad + 4A_4x^3], \end{aligned} \quad (39)$$

from which we can see once again that there may not exist certain symmetrical points including origin, where approximate resultant forces are identical with exact ones, as long as  $A_3$  is not zero.

If boundary conditions at both ends and loading are symmetric with respect to  $x = 0$ , the bending moment distributions in Eqs. (34) and (38) will be symmetric, too. The symmetric bending moment distributions lead to  $A_3 = 0$ , so the approximate shear force will be always exact at the origin. But, in general, the bending moment distribution is not symmetric. Even when the moment distribution in a beam is symmetric, the moment distribution in an element will be not symmetric if the beam is modelled by more than a single element. Therefore, a cantilever beam will be considered in the later subsections 4.2 & 4.3 to lead the discussions without loss of generality.

## 4. Examples and Discussion

### 4.1 Description of rigid body motion

In the section 3, we have shown that the single

unconstrained beam element describes the rigid body motions correctly. In this subsection, we will prove explicitly that the beam discretized by the beam elements also describe the rigid body motions correctly.

Since the beam element under consideration is 2-noded element, its Jacobian determinant is constant. So, the error-moment equations in Eqs. (17) and (18) can be rewritten as follows in the non-dimensional local coordinate  $\xi$  ( $-1 \leq \xi \leq +1$ ) as shown in Fig. 2.

$$\int_{-1}^{+1} (x - x_{\text{exact}}) d\xi = 0, \quad (40)$$

and

$$\int_{-1}^{+1} (x - x_{\text{exact}}) \xi d\xi = 0. \quad (41)$$

Assume the displacement function of an element ( $k$ ) shown in Fig. 3 as

$$w^{(k)} = a_0^{(k)} + a_1^{(k)} \xi_k + a_2^{(k)} \xi_k^2 + a_3^{(k)} \xi_k^3, \quad (42)$$

where the superscripts in parentheses denote element ( $k$ ) and  $\xi_k$  denotes the local coordinate of the element ( $k$ ).

The rigid body motions of the unconstrained meshes as shown in Fig. 3(a2) and (b2) can be easily obtained as follows :

(1) Unconstrained two-mesh test

The rigid body motions of the unconstrained single elements (1) and (2) as shown in Fig. 3(a1) are obtained from Eqs. (40) and (41) as follows : For the element (1) in Fig. 3(a1),

$$w^{(1)} = a_0^{(1)} + a_1^{(1)} \xi_1, \quad (43)$$

$$\theta^{(1)} = a_1^{(1)}. \quad (44)$$

and for the element (2) in Fig. 3(a1),

$$w^{(2)} = a_0^{(2)} + a_1^{(2)} \xi_2, \quad (45)$$

$$\theta^{(2)} = a_1^{(2)}. \quad (46)$$

By using the compatibility at the node 2 in Fig. 3(a2) such as

$$w^{(1)}|_{\xi_1=+1} = w^{(2)}|_{\xi_2=-1}, \quad (47)$$

$$\theta^{(1)}|_{\xi_1=+1} = \theta^{(2)}|_{\xi_2=-1}, \quad (48)$$

we obtain the rigid body motions of the element (2) in two-mesh

$$w^{(2)} = (a_0^{(1)} + 2a_1^{(1)}) + a_1^{(1)} \xi_2, \quad (49)$$

$$\theta^{(2)} = a_1^{(1)}. \quad (50)$$

Note that the rigid body motions of the element (2) in two mesh are also expressed by the same degree of freedoms of element (1). This implies that the two-mesh also can describe the rigid body motions as the single unconstrained element can. Therefore, the two-mesh can describe the rigid body motions correctly.

(2) Unconstrained three-mesh test

The rigid body motions of the element (2) in the unconstrained two-mesh shown in the left of Fig. 3(b1) are given in Eqs. (49) and (50) and the rigid body motions of the single unconstrained element (3) in the right of Fig. 3(b1) are given as

$$w^{(3)} = a_0^{(3)} + a_1^{(3)} \xi_3, \quad (51)$$

$$\theta^{(3)} = a_1^{(3)}. \quad (52)$$

By using the compatibility at the node 3 shown in Fig. 3(b2) such as

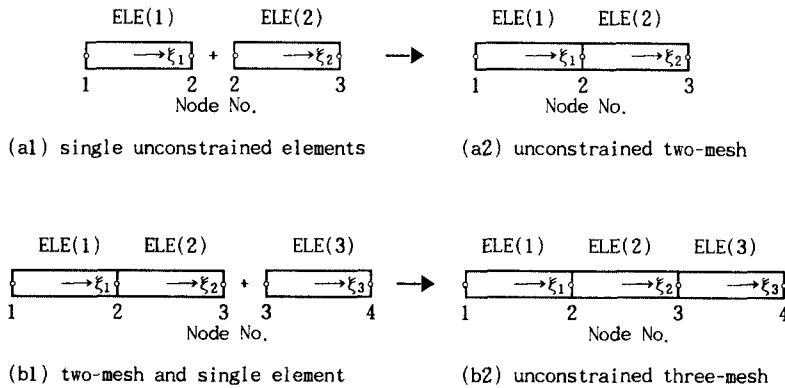


Fig. 3 Unconstrained elements and meshes

$$w^{(2)}|_{\xi_2=+1} = w^{(3)}|_{\xi_3=-1}, \quad (53)$$

$$\theta^{(2)}|_{\xi_2=+1} = \theta^{(3)}|_{\xi_3=-1}, \quad (54)$$

we obtain the rigid body motions of the element (3) in three-mesh such as

$$w^{(3)} = (a_0^{(1)} + 4a_1^{(1)}) + a_1^{(1)}\xi_3, \quad (55)$$

$$\theta^{(3)} = a_1^{(1)}. \quad (56)$$

Once again, the rigid body motions of the element (3) in the three mesh are also expressed by the same degree of freedoms of element (1). This implies that the three-mesh can describe the rigid body motions as the single unconstrained element can. Therefore, the mesh shown in Fig. 3(b2) can describe the rigid body motions correctly.

From the above examples, we see that a mesh discretized by the beam elements can describe the rigid body motion correctly.

**4.2 Error distribution depending on the order of loading**

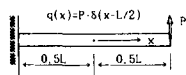
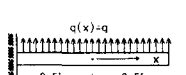
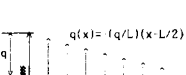
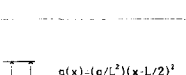
We shall consider the errors of approximate deformation fields and the errors of force resultants when cantilevered beams are modelled by a single Hermite element of degree three. The errors of approximate quantities of the beams, which are

obtained by erro-moment equations, are tabulated in Table 1 for typical loadings. Table 1 shows that the approximate kinematic variables are exact at nodal points irrespective of the order of loading  $q(x)$ . But the approximate force resultants do not have a consistent rule on the locations where they are identical with exact ones. The approximate force resultants are compared with exact ones for beams of length  $L=10$  in Fig. 4, which shows forllowing facts.

(1) For a uniformly distributed force, the moment is exact only at  $x = \pm(1/3)^{0.5}(L/2)$  and shear force is exact only at the origin,  $x=0$ .

(2) For linearly- or quadratically-distributed force, the points on which the approximate resultant forces are identical with exact ones do not agree with the Gauss points. These points are called true bending point and true shear force point, respectively. The distance of the true bending moment points from the Gauss points ( $x = \pm(1/3)^{0.5}(L/2)$ ) increases as the order of loading increases. The distance of true shear force point from the origin ( $x=0$ ) also increases as the order of loading  $q(x)$  increases.

**Table 1** The error distribution of approximate solutions depending on the order of load  $q(x)$

Model	Exact Solutions	Approximate Solutions	Error Distributions
 <p><math>q(x) = P \cdot \delta(x-L/2)</math></p>	$W_{\text{exact}} = (P/6EI)(-x^3 + 3Lx^2/2 + 9L^2x/4 - 5L^3/8)$ $\theta_{\text{exact}} = (P/6EI)(-3x^2 + 3Lx + 9L^2/4)$ $M_{\text{exact}} = (P/6)(-6x + 3L)$ $V_{\text{exact}} = -P$	same as exact solutions	$W - W_{\text{exact}} = 0$ $\theta - \theta_{\text{exact}} = 0$ $M - M_{\text{exact}} = 0$ $V - V_{\text{exact}} = 0$
 <p><math>q(x) = q</math></p>	$W_{\text{exact}} = (q/24EI)(x^4 - 2Lx^3 + 3L^2x^2/2 + 7L^3x/2 + 17L^4/16)$ $\theta_{\text{exact}} = (q/24EI)(4x^3 - 6Lx^2 + 3L^2x + 7L^3/2)$ $M_{\text{exact}} = (q/24)(12x^2 - 12Lx + 3L^2)$ $V_{\text{exact}} = (q/24)(24x - 12L)$	$w = (q/24EI)(-2Lx^3 + 2L^2x^2 + 7L^3x/2 + L^4)$ $\theta = (q/24EI)(-6Lx^2 + 4L^2x + 7L^3/2)$ $M = (q/24)(-12Lx + 4L^2)$ $V = (q/24)(-12L)$	$W - W_{\text{exact}} = -(q/24EI)(x^2 - (L/2)^2)^2$ $\theta - \theta_{\text{exact}} = -(q/24EI)[4x(x^2 - (L/2)^2)]$ $M - M_{\text{exact}} = -(q/24)[12(x^2 - (L/2)^2)/3]$ $V - V_{\text{exact}} = -(q/24)(24x)$
 <p><math>q(x) = (q/L)(x-L/2)</math></p>	$W_{\text{exact}} = (q/120EIL)(-x^5 + 5Lx^4/2 - 5L^2x^3/2 + 5L^3x^2/4 - 75L^4x/16 + 49L^5/32)$ $\theta_{\text{exact}} = (q/120EIL)(-5x^4 + 10Lx^3 - 15L^2x^2/2 + 5L^3x/2 + 75L^4/16)$ $M_{\text{exact}} = (q/120L)(-20x^3 + 30Lx^2 - 15L^2x + 5L^3/2)$ $V_{\text{exact}} = (q/120L)(-60x^2 + 60Lx - 15L^2)$	$w = (q/120EIL)(-3L^2x^3 + 5L^3x^2/2 + 19L^4x/4 + 11L^5/8)$ $\theta = (q/120EIL)(-9L^2x^2 + 5L^3x + 19L^4/4)$ $M = (q/120L)(-18L^2x + 5L^3)$ $V = (q/120L)(-18L^2)$	$W - W_{\text{exact}} = (q/120EIL)(x^2 - (L/2)^2)^2 \cdot (x - 5L/2)$ $\theta - \theta_{\text{exact}} = (q/120EIL)(x^2 - (L/2)^2) \cdot (5x^2 - 10Lx - L^2/4)$ $M - M_{\text{exact}} = (q/120L)[20x(x^2 - 3(L/2)^2)/5 - 30L(x^2 - (L/2)^2)/3]$ $V - V_{\text{exact}} = (q/120L)(60x^2 - 60Lx - 3L^2)$
 <p><math>q(x) = (q/L^2)(x-L/2)^2</math></p>	$W_{\text{exact}} = (q/360EIL^2)\{(x-L/2)^6 + 6L^3(x-L/3)\}$ $\theta_{\text{exact}} = (q/360EIL^2)\{6(x-L/2)^3 + 6L^3\}$ $M_{\text{exact}} = (q/360L^2)\{30(x-L/2)^4\}$ $V_{\text{exact}} = (q/360L^2)\{120(x-L/2)^3\}$	$w = (q/360EIL^2)(-4L^3x^3 + 3L^4x^2 + 6L^3x + 7L^5/4)$ $\theta = (q/360EIL^2)(-12L^3x^2 + 6L^4x + 6L^5)$ $M = (q/360L^2)(-24L^3x + 6L^4)$ $V = (q/360L^2)(-24L^3)$	$W - W_{\text{exact}} = (q/360EIL^2)(x^2 - (L/2)^2)^2 \cdot (-x^2 + 3Lx - 17L^2/4)$ $\theta - \theta_{\text{exact}} = (q/360EIL^2)(x^2 - (L/2)^2) \cdot (-6x^3 + 15Lx^2 - 33L^2x/2 - 3L^3/4)$ $M - M_{\text{exact}} = (q/360L^2)\{-30(x^4 - (L/2)^4)/5 + 60Lx(x^2 - 3(L/2)^2)/5 - 45L^2(x^2 - (L/2)^2)/3\}$ $V - V_{\text{exact}} = (q/360L^2)(-120x^3 - 180Lx^2 - 90L^2x - 9L^3)$

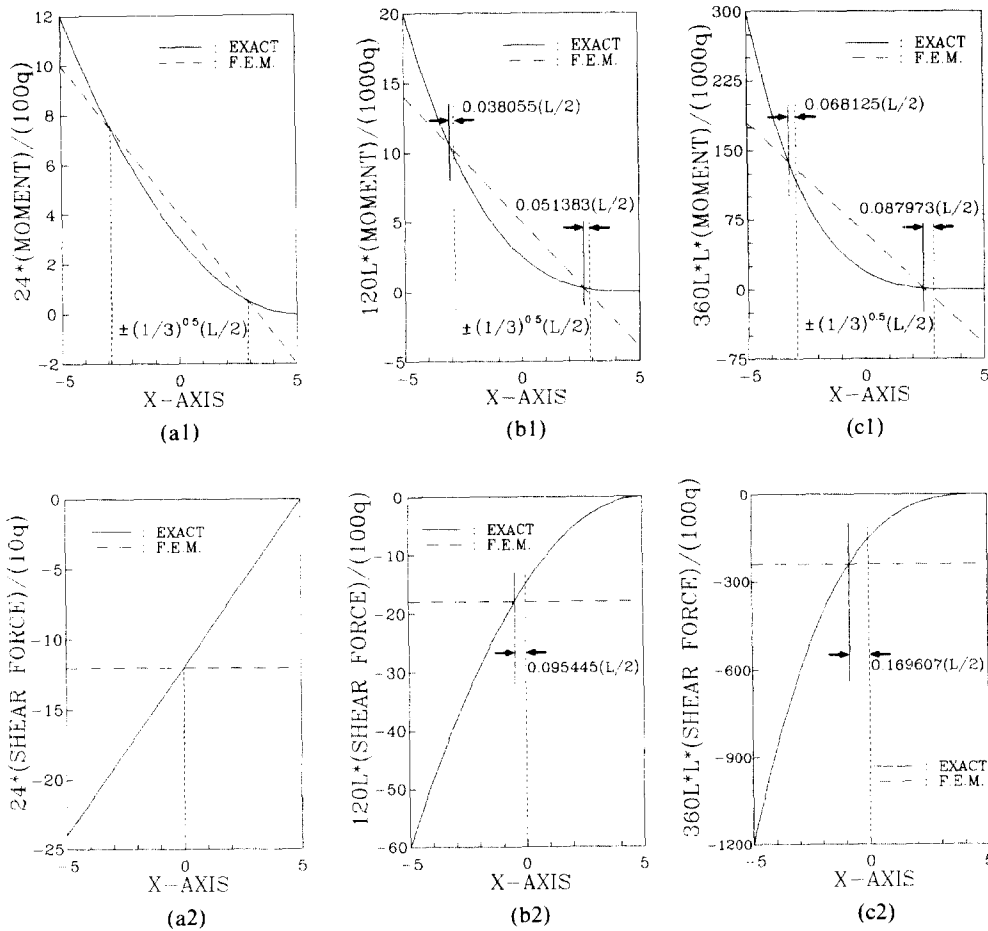


**Fig. 4** Distributions of bending moments(a1, b1, c1) and shear forces (a2, b2, c2) where (a1) & (a2) for uniformly distributed load, (b1) & (b2) for linearly distributed load, and (c1] & (c2) for quadratically distributed load (refer to Table 1)

**4.3 Optimal points in the limit sense**

In this section, we will show that the so-called optimal points mean the points to which the true resultant forces' points converge as the number of elements increases. Moan compared pointwise error of principal derivative at optimal points with those at the point where maximum error occurs, usually at the ends of an element. His comparison seems to be insufficient to show that the error of a principal derivative is minimal at the optimal points, because the pointwise error at certain points in terms of number of elements does not show directly that the true resultant forces' points approach to his optimal points.

The convergence of true resultant forces' points to optimal points will be shown as the number of elements increases for the cantilever as shown in Fig. 5, in which  $\xi_{nk}$  is the nondimensional element coordinates of  $k$ -th element when the beam is discretized with  $n$  equal-sized elements. By using error-moment equations in Eqs. (40) and (41), the true resultant forces' points of the first elements (ELE. 1 of Fig. 5) are calculated as the number of elements increases. Figure 6 shows the convergence of true bending moment points to the optimal points ( $\xi_{n1} = \pm(1/3)$ ,  $n = 1, 2, 4, 8$ ), and Fig. 7 shows the convergence of true shear force point to its optimal point ( $\xi_{n1} = 0$ ,  $n = 1, 2, 4, 8$ ) as

the number of element increases.

**4.4 Discussion**

For the one-dimensional boundary problem, the errors of FE analysis are of two types :

(1) Errors due to the numerical evaluation of the integrals and the use of the computer performing the numerical calculations.

(2) Errors due to the approximate character of the finite element formulation.

In this paper, the error resulting from the use of the computer or from the hand calculation is ruled out by obtaining the FE results using the error-moment equations. So all the errors presented in the previous section can be considered to be of type 2.

From the results of examples, we can see that the Hermite polynomial of degree three can describe the nodal displacements ( $w, \theta$ ) exactly irrespective of the order of loading  $q(x)$ . But its descriptive capability for bending moments and shear forces deteriorates as the order of curvature field increases. Consequently, the error of  $M$  and  $V$  sampled at their optimal points respectively may increase as the order of loading  $q(x)$  increases. Thus, in order to improve the accuracy of approximate solutions, a finer discretization is required because a finer discretization makes it possible that the curvature field within a single element be approximated with sufficient accuracy irrespective of the order of loading, as shown in Figs. 6 and 7. This is particularly significant in that the design of a structure is usually dictated by the values of the force resultants ( $M$  and  $V$ ) rather than by the kinematical variables ( $w$  and  $\theta$ ), making it necessary to have accurate estimates of  $M$  and  $V$ .

Figure 4 may be regarded as a pattern showing

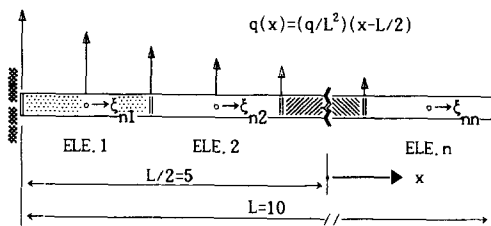
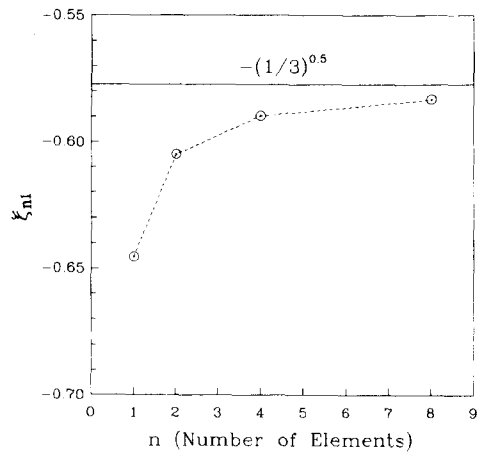
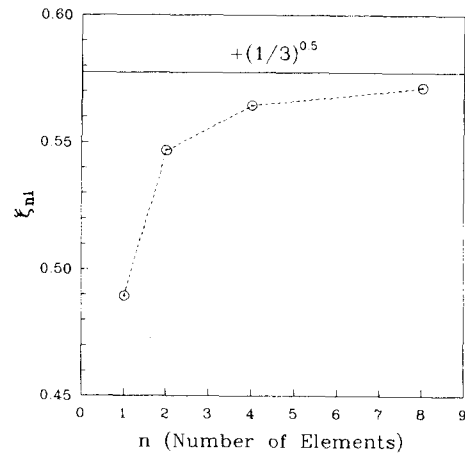


Fig. 5 Discretization of cantilever



(a) Convergence to  $\xi_{n1} = (1/3)^{0.5}$



(b) Convergence to  $\xi_{n1} = -(1/3)^{0.5}$

Fig. 6 Convergence of true bending moment points

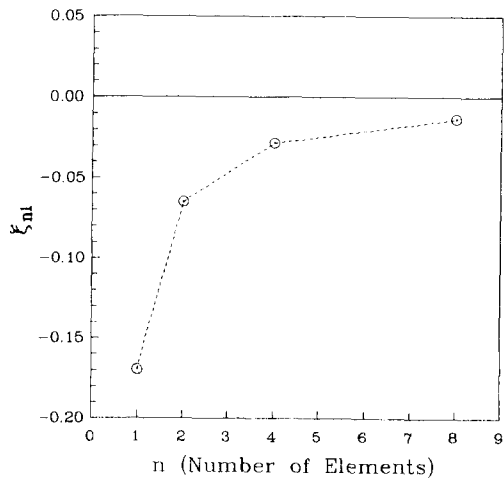


Fig. 7 Convergence of true shear force points



the convergence of approximate resultant forces' points to their optimal points, i.e., the shift of (c)  $\rightarrow$  (b)  $\rightarrow$  (a) in Fig. 4 may represent a convergence pattern as the number of elements increases. In this limit sense, the Gauss points can be regarded as the optimal locations of bending moment and the origin may be regarded as the optimal point of shear force. The optimal location in the limit sense is contrasted with that of  $C^0$ -continuous beam element, that is, the optimal point of  $C^0$ -continuous beam element (Min and Kim, 1991) is the location where locking due to spurious constraint is alleviated.

## 5. Conclusion

By using the error-moment equations which are derived from energy functional, the following performance of the thin beam Hermite element of degree three is examined :

- (1) Descriptive capability for rigid body motions.
- (2) Descriptive capability for a deformation depending on the order of loading.
- (3) The numerical implication of the optimal points.

The single unconstrained beam element is able to describe the rigid body motions correctly without zero energy modes when analytical integration or 2-point Gaussian quadrature is employed. So, the mesh discretized with the elements can describe the rigid body motions correctly without zero energy modes, too.

To examine the descriptive capability for deformation, the Hermite polynomial of degree three was tested for the beam subjected to constant, linear, and quadratic curvature fields. The results show that the accuracy of the moments and the shear forces associated with higher-order loading

$q(x)$  suffers from the lack of its descriptive capability while the kinematic variables at nodal points are exact irrespective of the order of loading. So, as the order of loading  $q(x)$  increases, a finer discretization is required not only because the finer discretization reduces the maximum error of the force resultants within an element but also because it makes the true resultant forces' points converge to their optimal points. In relation to the latter, the optimal stress points suggested by Barlow can be re-interpreted as the optimal points in the limit sense.

## References

- Barlow, J. 1976, "Optimal Stress Locations in Finite Element Models," *Int. J. Numer. Meth. Engng.*, Vol. 10, pp. 243~251.
- Bickford, W.B., 1990, *A First Course in the Finite Element Method*, R.R. Donnelley & Sons Company, Boston.
- Hinton, E. and Campbell, J. S., 1974, "Local and Global Smoothing of Discontinuous Finite Element Functions Using a Least Squares Method," *Int. J. Numer. Meth. Engng.* Vol. 8, pp. 461~480.
- Min Oak-key and Kim Yong-woo, "Reduced Minimization Theory in Beam Elements," *Int. Numer. Meth. Engng.* in Press.
- Moan, T., 1973, "On the Local Distribution of Errors by Finite Element Approximations," *Theory and Practice in Finite Element Structural Analysis*, University of Tokyo Press.
- Ralston, A. 1965, *A First Course in Numerical Analysis*, McGRAW-Hill Book Company, New York.
- Zienkiewicz, O.C., 1977, *The Finite Element Method*, McGRAW-Hill Book Company, London.